Respiratory Research

RESEARCH Open Access

CT-based whole lung radiomics nomogram for identification of PRISm from non-COPD subjects

TaoHu Zhou[1,2†], Yu Guan[1†], XiaoQing Lin[1,3†], XiuXiu Zhou[1], Liang Mao[4], YanQing Ma[5], Bing Fan[6], Jie Li[1,3], ShiYuan Liu[1] and Li Fan[1*]

Abstract

Background Preserved Ratio Impaired Spirometry (PRISm) is considered to be a precursor of chronic obstructive pulmonary disease. Radiomics nomogram can effectively identify the PRISm subjects from non-COPD subjects, especially when during large-scale CT lung cancer screening.

Methods Totally 1481 participants (864, 370 and 247 in training, internal validation, and external validation cohorts, respectively) were included. Whole lung on thin-section computed tomography (CT) was segmented with a fully automated segmentation algorithm. PyRadiomics was adopted for extracting radiomics features. Clinical features were also obtained. Moreover, Spearman correlation analysis, minimum redundancy maximum relevance (mRMR) feature ranking and least absolute shrinkage and selection operator (LASSO) classifier were adopted to analyze whether radiomics features could be used to build radiomics signatures. A nomogram that incorporated clinical features and radiomics signature was constructed through multivariable logistic regression. Last, calibration, discrimination and clinical usefulness were analyzed using validation cohorts.

Results The radiomics signature, which included 14 stable features, was related to PRISm of training and validation cohorts ($p < 0.001$). The radiomics nomogram incorporating independent predicting factors (radiomics signature, age, BMI, and gender) well discriminated PRISm from non-COPD subjects compared with clinical model or radiomics signature alone for training cohort (AUC 0.787 vs. 0.675 vs. 0.778), internal (AUC 0.773 vs. 0.682 vs. 0.767) and external validation cohorts (AUC 0.702 vs. 0.610 vs. 0.699). Decision curve analysis suggested that our constructed radiomics nomogram outperformed clinical model.

Conclusions The CT-based whole lung radiomics nomogram could identify PRISm to help decision-making in clinic.

Key message

What is already known on this topic Identifying PRISm subjects among non-COPD subjects, especially in the context of large-scale CT lung cancer screening, is currently a challenge.

†TaoHu Zhou, Yu Guan and XiaoQing Lin contributed equally to this work.

*Correspondence:
Li Fan
fanli0930@163.com

Full list of author information is available at the end of the article

What this study adds In this retrospective, and multicentric study that included 1481 subjects, radiomics nomogram developed by integrating radiomics signature and clinical features achieved good performance for the identification of PRISm, with AUC of 0.787, 0.773 and 0.702 in training, internal and external validation cohort.

How this study might affect research, practice or policy Radiomics nomogram, as a promising tool for identifying the PRISm from non-COPD subjects, hold great potential for guiding timely treatment and showing the added value of chest CT to evaluate the lung function status besides the morphological evaluation, especially during large-scale CT lung cancer screening.

Keywords PRISm, Radiomics, Computed tomography, Nomogram

Introduction

Chronic obstructive pulmonary disease (COPD) is a primarily factor causing morbidity and mortality globally, ranking the third leading cause of death globally and resulting in tremendous health care, social and economic burdens [1–3]. The COPD burden may be significantly increased in the future decades owing to rapid aging of Chinese population. According to recent demographic data from the National Bureau of Statistics of China, the proportion of the population aged 65 and above is expected to increase from 12.6% in 2020 to a projected 28.1% by 2050 [4]. This rapid aging trend could significantly heighten the COPD burden in China compared to other populations. A recent meta-analytic study revealed that the prevalence of COPD increases notably with age with a marked rise from 4.37% (95% CI 2.76% – 6.33%) among individuals aged 40–49 years to 24.03% (95% CI 20.04%-28.26%) in those aged 70 years and older [5]. Moreover, it has been reported China had the largest absolute economic burden of COPD in the world, China alone accounts for 83.5% of the economic losses in upper-middle-income countries [6]. Screening and identifying COPD early can prevent disease progression and reduce health and economic burdens.

Preserved ratio impaired spirometry (PRISm), also known as restrictive pattern or unclassified spirometry, is defined as a FEV1 of less than 80% predicted, despite a normal or preserved FEV1/forced vital capacity (FVC) ratio (≥0.70) [7]. PRISm can transition to normal, obstructive or restrictive spirometry over time [8]. Therefore, PRISm has been increasingly identified with prognostic significance [9–12]. Based on some population-based studies performed in Western populations, PRISm subjects are associated with an increased airflow limitation (AFL) rate and an increased mortality risk relative to subjects having normal lung function [9–12]. These observations are similar to those reported from the Asian region [13]. According to the community survey involving 3032 Japanese people during the 5-year follow-up [13], 31 with PRISm at the first visit showed an increased overall mortality and a higher probability of COPD progression compared with people showing normal spirometry. As a result, finding markers that can accurately identify PRISm and offer a foundation for early prognosis prediction is of great significance for enhancing the management of clinical subjects.

Despite PFTs remaining the gold standard for diagnosing PRISm, the utilization rate is relatively low. In China, only 6.7% of individuals over 40 have undergone PFTs, resulting in a significant number of undiagnosed cases due to limited accessibility [14]. Imaging, particularly chest CT scans, offer considerable advantages and potential. With the widespread adoption of lung cancer screening programs, not only the use of CT scans are increased but also CT could provide more detailed anatomical information. Results from large-scale screening studies such as NELSON and NLST have shown reduced mortality rates of lung cancer undergoing lung cancer CT screenings [15]. These advancements offer greater survival chances for cancer patients. If we can simultaneously screen for PRISm during lung cancer screenings could provide more timely medical interventions and more benefit for the population [16].

In recent years, radiomics has aroused increasing attention, which refers to the process in which medical images are converted in high-dimensional, mineable data through high-throughput quantitative feature extraction and data analysis to support decision-making [17]. Radiomics is adopted for identifying chest diseases and evaluating prognosis [18–22]. Recently, several imaging studies have focused on exploring those imaging features of PRISm and the significance of quantitative HRCT in early diagnosis. However, to our best knowledge, studies have not yet investigated the relationship between radiomics and PRISm. The purpose of the study was to investigate the performance of CT radiomics in identifying PRISm subjects among non-COPD subjects with one-stop CT screening.

Methods

Subjects

Totally 1513 subjects with PFT in five hospitals were retrospectively recruited between February 2013 and December 2022. The trial was registered in Chinese Clinical Trial Registry on 29 March 2023 (Number: ChiCTR2300069929, URL: https://www.chictr.org.cn/

showproj.html?proj=192439). Subjects were enrolled based on the following inclusion criteria: (1) both chest CT and PFT were performed in the same hospital; (2) the PFT to chest CT interval less than 2 weeks; (3) complete thin-section (<2 mm) chest CT images; (4) the post-bronchodilator FEV1/FVC≥0.7. The exclusion criteria as follows: (1) co-morbid other thoracic disease (e.g., pneumonia, pulmonary atelectasis, lung nodules larger than 6 mm or masses, asthma, and pleural effusion); (2) concomitant malignant neoplasms; and (3) artifacts. Finally, 1481 subjects were included in the study. Among them, 1234 subjects from one hospital were randomly divided into training (n=864) and internal validation cohort (n=370) with the ratio of 7:3, using "caret" R package. Those from other four hospitals were classified in independent external validation cohort (n=247). Figure 1 displays the subjects screening workflow. In the meanwhile, clinical basic information of the subjects such as age, sex, height, weight, BMI, and smoking status, was obtained based on electronic medical records system. The approval of the retrospective study was provided by the institutional review board of the leading hospital. Due to the retrospective nature, the informed consent was waived.

CT image acquisition and pulmonary function test

Table S1 shows the CT acquisition parameters and pulmonary function test apparatus in detail. Lung function was categorized in line with modified GOLD criteria and prior studies [12, 23]. In this study, based on the PFT results, the non-COPD subjects were classified into the PRISm and normal spirometry groups for the training, internal validation and the independent external validation cohorts. Normal spirometry was defined as FEV1/FVC≥0.70 and FEV1≥80% predicted; PRISm was defined as FEV1/FVC≥0.70 and FEV1<80% predicted.

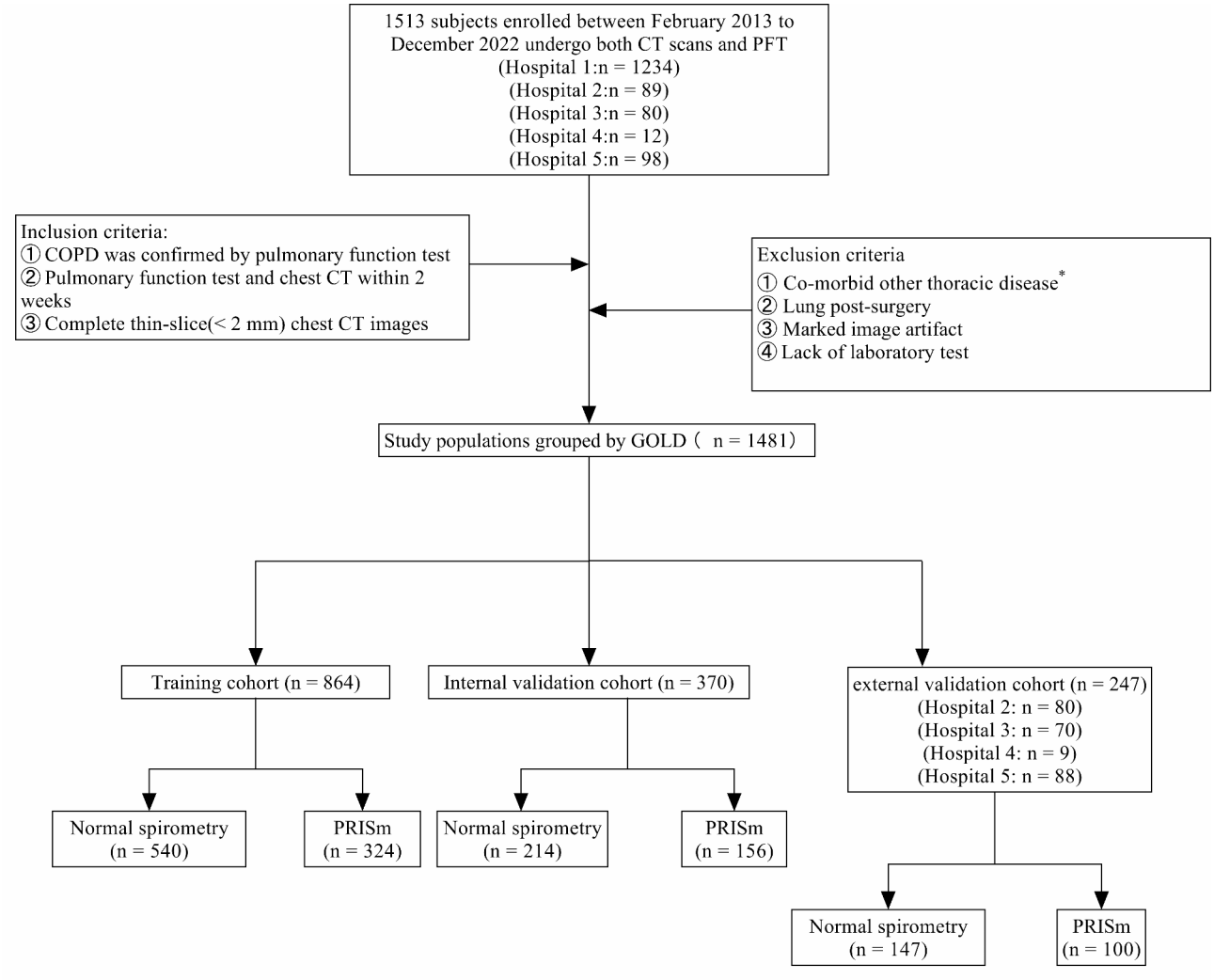

Fig. 1 Flowchart for the selection of the study population

Whole lung CT segmentation, radiomics features extraction and selection

The pretrained CNN of U-Net structure was used to process chest CT images of each subject [24]. Firstly, the right and left lungs were automatically segmented using a publicly accessed deep-learning model, U-net (R231) (https://github.com/JoHof/lungmask), which has been trained based on different large-scale datasets including broad visual variability. Secondly, we merged the right and left lung into a combined region of interest (ROI) (Figure S1). Thirdly, an experienced chest radiologist with 8-year experience examined the segmentation outcome visually with the use of ITK-SNAP software (version 3.8.0, www.itksnap.org). Inaccurate segmentation could be corrected manually with ITK-SNAP.

Prior to the extraction of radiomics features, three steps were utilized for image preprocessing. Firstly, linear interpolation was employed to resample images to 1 mm*1 mm*1 mm. Secondly, gray-level discretization was used for converting continuous images to discrete integer values and a bin width of 25 was used to reduce the effect of imaging noise. At last, wavelet and log image filters were adopted for eliminating mixed noise during image digitization and obtaining high- or low-frequency features. Pyradiomics software (version 3.0.1, https://pyradiomics.readthedocs.io/en/latest/) was adopted for extracting lung radiomics features. Totally 1218 features were obtained in each volume of interest with open-source package (pyradiomics), including first-order, gray-level cooccurrence matrix (GLCM), gray-level run length matrix (GLRLM), gray-level size zone matrix (GLSZM), gray-level dependence matrix (GLDM), and shape features. Radiomics features comply with the image biomarker standardization initiative (IBSI) [25], including standardization of acquisition and feature extraction, guidelines for annotation, segmentation, feature selection, model building and validation and clinical implementation. For the purpose of normalizing the features, the Z score method was adopted. In addition, the difference in the numerical scale was removed.

Optimal radiomics features were selected. Firstly, by eliminating redundancy with correlation coefficient > 0.90, we selected the optimal radiomic feature. Secondly, maximal redundancy minimal relevance (mRMR) algorithm was adopted for eliminating irrelevant or redundant features. mRMR has been demonstrated to be an efficient and reliable feature selection method for radiomics which can discover the optimal subset of features through considering the importance of features and the correlation between them. Least absolute shrinkage and selection operator (LASSO), which is the embedded approach, has been extensively applied to select high-dimensional radiomics features [26]. In addition, 10-fold cross-validation was carried out using penalty parameter and LASSO regression algorithm. The best feature dataset that had the lowest cross-validation binomial deviation was chosen, while nonzero coefficient was defined as selected feature weight, representing relation of features with PRISm. We used a linear combination of selected feature and coefficient vectors to calculate the Radscore of each subject. In addition, the construction of radiomics model was made.

Model, nomogram construction and performance evaluation

Three models were built including clinical, radiomic and the combined models. Statistically significant risk variables were identified through univariable logistic regression, which were then incorporated for multivariable regression to construct the clinical and combined models. Last, we constructed a nomogram to visualize the combined model, graphically evaluated the variable importance and calculate the prediction accuracy. AUCs (areas under the ROC curve) of those three models were compared using Delong test. Nomogram calibration was assessed through calibration curves (Hosmer-Lemeshow test). Nomogram clinical practicability was assessed by decision curves Analysis (DCA).

Statistical analysis

In statistical analysis, R software (version 4.2.2; http://www.Rproject.org) and IBM SPSS Statistics (Version 26.0; IBM Corp., New York, USA) were used. Measurement data were represented through mean ± standard deviation. Continuous variables of normal distribution were evaluated with the use of Mann-Whitney/Wilcoxon nonparametric test. Categorical data were explored by chi-square test between groups. Independent predicting factors were determined from diverse clinical variables by multivariate logistic regression. $P<0.05$ represented statistical significance. "glmnet" package was used for LASSO analysis. In addition, we employed "caret" package for random division. "rms" package was applied for drawing calibration plot and conducting multivariate logistic regression. "pROC" package was used for drawing ROC (receiver operating characteristic curve) of radiomics signature. "rmda" package for DCA to evaluate net benefit, which is defined as the differential value of true positives proportion and false positives proportion, weighted by the relative harm of false positive and false negative results.

Results

Demographic data and clinical model establishment

Table 1 displays basic demographic features of subjects. A total of 864 subjects with normal spirometry were in training cohort (500 males, 364 females; average age, 60.3 ± 12.7 years), 370 subjects were in internal validation

Table 1 Characteristics of subjects with normal lung function in each cohort

Variables		Training Cohort ($N=864$)		*p*-value	Internal Validation Cohort ($N=370$)		*p*-value	External Validation Cohort ($N=247$)		*p*-value
		normal spirometry	PRISm		normal spirometry	PRISm		normal spirometry	PRISm	
Age		58.6 (12.3)	63.2 (12.7)	<0.001	58.3 (12.2)	64.3 (10.4)	<0.001	61.8(0.98)	61.2(1.3)	0.949
Gender				<0.001			0.003			0.014
	Male	272 (50.4)	228 (70.4)		105 (49.1)	102 (65.4)		88(59.9)	75(75.0)	
	Female	268 (49.6)	96 (29.6)		109 (50.9)	54 (34.6)		59(40.1)	25(25.0)	
Height		161.4 (7.8)	163.3 (8)	0.0006	161.3 (8.1)	172.4 (120.5)	0.178	164.2(0.7)	165.4(0.9)	0.309
Weight		62.8 (10.7)	67.5 (12.5)	<0.001	62.3 (9.6)	66.9 (13.8)	0.0002	63.0(0.8)	68.3(1.6)	0.008
BMI		24 (3.2)	25.3 (4.2)	<0.001	23.9 (2.8)	25 (4.7)	0.005	23.4(0.3)	24.8(0.5)	0.026
Smoking status				0.0003			0.0002			0.567
	Current Smoker	84 (15.6)	67 (20.7)		28 (13.1)	44 (28.2)		74(50.3)	44(44.0)	
	Former Smoker	36 (6.7)	43 (13.3)		17 (7.9)	19 (12.2)		30(20.4)	21(21.0)	
	Non-smoker	420 (77.8)	214 (66.0)		169 (79.0)	93 (59.6)		43(29.3)	35(35.0)	

cohort (207 males, 163 females; average age, 60.9±11.8 years) and 247 subjects were in external validation cohort (163 males, 84 females; average age, 61.6±12.4 years). The rates of PRISm subjects were 37.5% (324 of 864), 42.2% (156 of 370), and 40.5% (100 of 247) of training, internal, and external validation cohorts, respectively. Three cohorts differed significantly regarding gender and BMI ($p<0.05$). Significant differences were found in training and internal validation cohorts with respect to age and smoking status ($p<0.001$), but not in external cohort. In addition, age distribution was not of significant difference between two validation cohorts. Table 1 displays results of univariate and multivariate logistic regression. Age, BMI, and gender identified from multivariable regression were included to develop the clinical model. Figure 2 presents ROC curves for clinical model. The corresponding AUCs were 0.675 (95% CI: 0.637, 0.712), 0.682 (95% CI: 0.627, 0.737) and 0.610 (95% CI: 0.538, 0.682) in training, internal and external validation cohorts, respectively.

Radiomics feature selection and radiomics signature

Among 1218 radiomics features extracted from chest CT images, 245 features exhibited high stability, and then were decreased to 30 features through minimum redundancy maximum relevancy. Finally, LASSO was conducted to select features (Fig. 3A, B), among which, those 14 features with highest importance were retained, as shown in Fig. 3C. The calculation formulas for Radscore are listed in **Supplementary Results**.

Figure 2 displays ROC curves for radiomics signature. The AUCs of our radiomics signature were 0.778 (95% CI: 0.746, 0.810), 0.767 (95% CI: 0.718, 0.815) and 0.699 (95% CI: 0.633, 0.766) for training, internal and external validation cohorts, respectively.

Radiomics nomogram construction and model performance evaluation

Radscore and clinical features were incorporated to develop the radiomics nomogram for training cohort (Fig. 4A). The calibration curve of the radiomics nomogram showed good consistence between the predicted and expected probabilities for PRISm (Fig. 4B, C, D). Meanwhile, upon Hosmer–Lemeshow test, their *P*-values were 0.9995, 0.4521, and 0.1049 for training, internal, and external validation cohorts, respectively, which revealed relatively excellent agreement between the nomogram prediction and the actual observation. Figure 2 shows ROC curves for radiomics nomogram. AUCs were used as an index of diagnostic accuracy; a higher AUC reflects greater accuracy. Its AUC, sensitivity, specificity, and accuracy were 0.787 (95% CI: 0.756, 0.818), 75.0%, 68.5%, and 70.9%; 0.773 (95%CI: 0.725, 0.821), 64.1%, 78.8%, and 71.6%; and 0.702 (95%CI: 0.636,0.767), 63.9%, 68.0%,

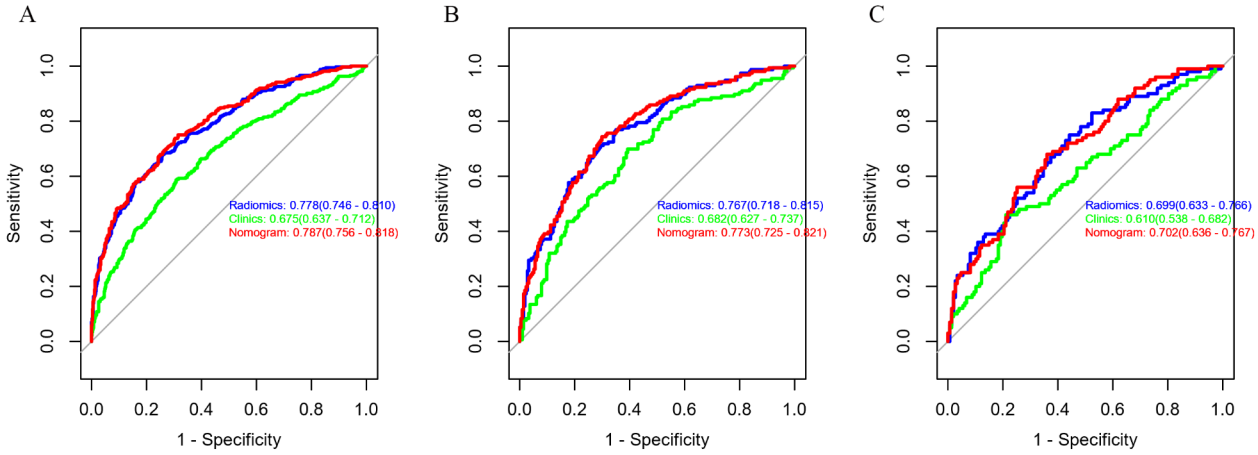

Fig. 2 Diagnostic performance of the clinical factors model, radiomics signature, and radiomics nomogram was assessed and compared through ROC curves in the training (**A**), internal validation (**B**) and external validation (**C**) cohorts. ROC = receiver operating characteristics; AUC = area under the receiver operating characteristic curve

and 65.6% in training, internal and external validation cohorts, separately.

Table 2 displays model diagnostic accuracy. Comparison between ROC curves was performed by the DeLong test. The Delong test showed that there was a statistically significant difference in AUCs between the radiomics nomogram and the clinical model (Z=6.64, $p<0.001$; Z=3.72, $p<0.001$; and Z=2.46, $p=0.014$ in the training, internal validation, and external validation cohort, respectively). There is a difference between the radiomics signature and radiomics nomogram (Z = -2.01, $p=0.044$) in the training cohort. But no significant difference (Z = -0.84, $p=0.401$ and Z=0.18, $p=0.855$ in internal validation, and external validation cohort, respectively) between the radiomics nomogram and radiomics signature. The correlation between radiomics signature and clinical model was the moderate in the training and internal validation cohorts ($R=0.4$). Correlations in the external validation cohort was weak ($R=0.2$).

Decision curve analysis was used to evaluate the clinical practicability of the nomogram prediction model (Fig. 4E). The results showed that the nomogram obtained more benefit than the "treat all," "treat none," and the clinical model when the threshold probability was in the range of 4–70%. An example of the nomogram in use is shown in Fig. 5. Similar to the points scoring system, we assigned points for each predictor of PRISm and then equated these predictors with the risk of PRISm. We can read the top score scale upward from the predictors to determine the points score associated with patient BMI, age, gender and the Radscore. Once a score has been assigned to each predictor, an overall score is calculated. Then, the total score is converted to the probability of PRISm by reading the associated probability of PRISm from the total point scale.

Discussion

Identifying subjects with PRISm is of great importance to verify the early, effective, and individualized decision-making in the prevention of COPD, because many PRISm would progress into COPD. In the present study, the radiomics nomogram incorporating clinical factors and radiomics signature was established and verified to identify PRISm subjects based on whole lung CT radiomics. The radiomics nomogram proposed in the current work exhibited favorable discrimination in training cohort (AUC, 0.787), internal validation cohort (AUC, 0.773) and external validation cohort (AUC, 0.702), outperforming radiomics signature (training, 0.778; internal validation, 0.767; external validation, 0.699) and clinical factor model (training, 0.675; internal validation, 0.682; external validation, 0.610).

The incidence and disease burden of COPD is high in China, the overall pulmonary function detection rate was still at a low level, and many people have been underdiagnosed. In contrast, the popularity of chest CT is very high, especially with the large-scale chest CT screening for lung cancer. Moreover, more and more community health service centers will be equipped with CT. Therefore, the most important clinical scenario is for the large-scale lung cancer screening population that usually does not perform PFT, and many people who were high risk (most likely to develop COPD) can be found through our model prediction, which can help enhance the early intervention of PRISm, reduce the social-economic burden and improve the patient's life quality. Many clinical factors have been explored in PRISm. It has been found female sex, old age, smoking, and extreme weight were related to PRISm [27]. The former and current smokers were examined in one cross-sectional and follow-up study of COPDGene [10, 28], as a result, PRISm

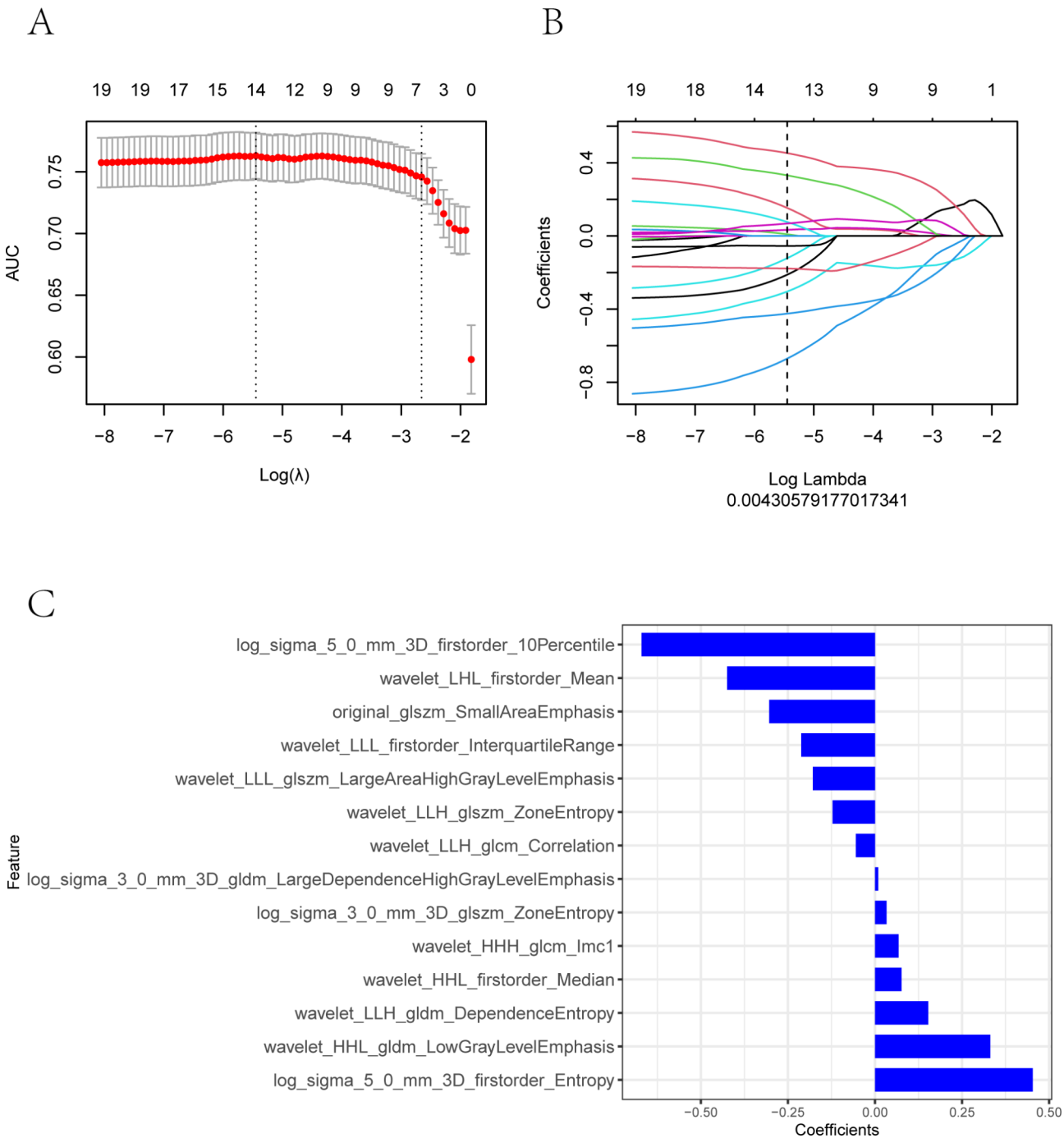

Fig. 3 Radiomics feature selection by using the least absolute shrinkage and selection operator (LASSO) logistic regression. (**A**) Selection of the tuning parameter (λ) in the LASSO model via 10-fold cross-validation based on minimum criteria. Binomial deviances from the LASSO regression cross-validation model are plotted as a function of log(λ). The y-axis shows binomial deviances and the lower x-axis the log(λ). Numbers along the upper x-axis indicate the average number of predictors. Red dots indicate average deviance values for each model with a given λ, and vertical bars through the red dots indicate the upper and lower values of the deviances. The vertical black lines define the optimal values of λ, where the model provides its best fit to the data. (**B**) The coefficients have been plotted vs. log(λ). (**C**) The 14 features with nonzero coefficients are shown in the plot

patients showed the increased BMI compared with COPD patients and normal subjects, while persistent smoking independently predicted the reduced life quality of COPD patients. Many studies suggest that age and BMI are imperative risk factors of PRISm [7]. The older cohorts may show an increased impaired spirometry rate, particularly through the longitudinal follow-up. BMI can induce the risk of PRISm risk through the distinct

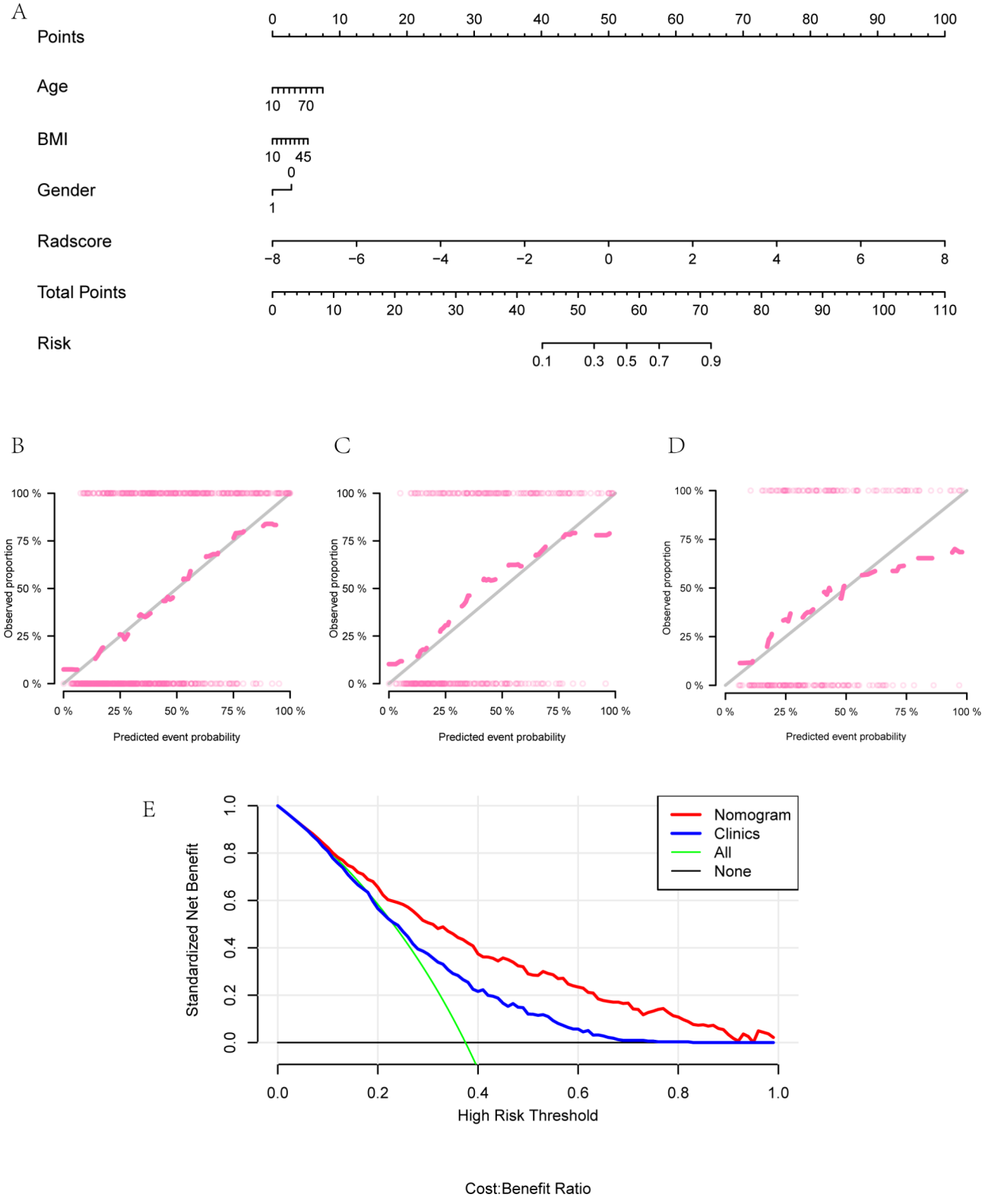

Fig. 4 Radiomics nomogram, calibration curves and DCA curves. (**A**) The radiomics nomogram, combining age, BMI, gender and Radscore, was developed in the training cohort. (B–D) The nomogram calibration curves in training (**B**), internal validation (**C**), and external validation (**D**) cohorts. Calibration curves indicate the goodness-of-ft of the model. (**E**) Decision curve analysis for different models

Table 2 Results of radiomics nomogram, radiomics signature, and the clinical factors model predictive ability for distinguishing between normal lung function and PRISm

Parameter		Cutoff	AUC (95% CI)	Sensibility	Specifcity
Clinical factors model	Training cohort	-0.35	0.675(0.637–0.712)	0.586	0.693
	Internal validation cohort		0.682(0.627–0.737)	0.557	0.696
	External validation cohort		0.610(0.538–0.682)	0.500	0.667
Radiomics signature	Training cohort	-0.53	0.778(0.746–0.810)	0.679	0.743
	Internal validation cohort		0.767(0.718–0.815)	0.667	0.743
	External validation cohort		0.699(0.633–0.766)	0.470	0.769
Radiomics nomogram	Training cohort	-0.68	0.787(0.756–0.818)	0.750	0.685
	Internal validation cohort		0.773(0.725–0.821)	0.640	0.788
	External validation cohort		0.702(0.636–0.767)	0.639	0.680

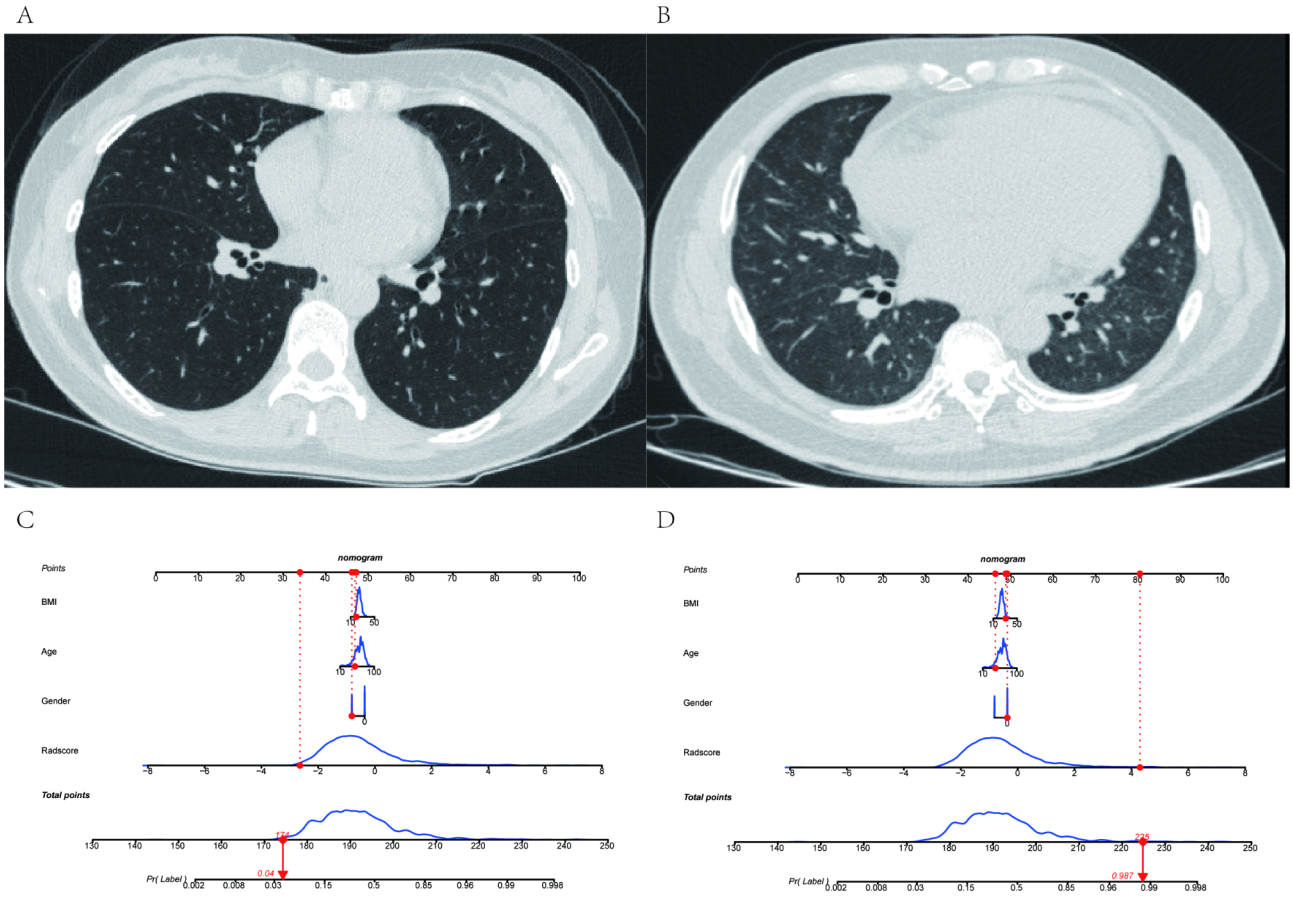

Fig. 5 An example of the nomogram in clinical practice. The nomogram was used to calculate the scoring process of risk of PRISm. (**A**) Thin-section chest CT image of a 49-year-old normal female subject. Her Clinical features were analyzed as follows: BMI = 19.5 kg/m2, Radscore = -2.64. The nomogram showed that this patient had a total of 174 points after summing all points, which corresponds to a close to 4.00% probability of PRISm. (**B**) Thin-section chest CT image of a 43-year-old male subject. His clinical features were analyzed as follows: BMI = 30.80 kg/m2, Radscore = 4.30. The nomogram showed that this patient had a total of 225 points after summing all points, which corresponds to a close to 96.9% probability of PRISm

pathway, including inflammatory and metabolic effects of adipose tissue [29]. Previous population-based studies suggest increased risk of restrictive pattern among females [30, 31]. In our study, age, sex and BMI were selected as independent predictors for PRISm subjects, Table 3 showed that female subjects with increased age and BMI are more likely to be PRISm, which was consistent with previous studies.

To the best of our knowledge, relevant studies are few on the identification of PRISm with CT-based methods. Wei et al. [32] evaluated the CT-based quantitative features with an in-house system, and found that lung capacity, emphysema index, and airway wall area did not predict intermediate-stage chronic bronchitis that progresses from normal lung function to early COPD. Moreover, their study did not evaluate CT textural

Table 3 Univariate and Multivariate logistic regression analysis

Variable	Univariate logistic regression			Multivariate logistic regression (Clinical model)			Multivariate logistic regression (Radiomics nomogram)		
	OR	95%CI	*P* value	OR	95%CI	*P* value	OR	95%CI	*P* value
Age	1.03	1.02–1.04	< 0.001	1.03	1.01–1.04	< 0.001	1.01	1.00-1.03	0.059
Height	1.03	1.01–1.05	< 0.001						
Weight	1.04	1.02–1.05	< 0.001						
BMI	1.10	1.06–1.14	< 0.001	1.08	1.04–1.13	< 0.001	1.02	0.98–1.07	0.37
Smoking	0.76	0.64–0.90	0.002						
Gender	0.43	0.32–0.57	< 0.001	0.48	0.36–0.65	< 0.001	0.64	0.46–0.89	0.008
Radscore	2.99	2.49–3.58	< 0.001	-	-	-	2.71	2.25–3.26	< 0.001

features and relevant clinical factors. To date, there are rare study for the identification of PRISm population using radiomics. The CT-based radiomics nomogram is established by integrating clinical factors and radiomics signature for identifying PRISm in our study. It is very difficult to identify the proper margin of the diffuse lung lesions. Thus, the full-automatic lung lobe segmentation method was performed using U-Net, which has been proven efficacy in pulmonary disease, especially pulmonary diffuse disease [33–36]. This radiomics signature included 14 radiomics features, which well distinguished PRISm subjects from normal spirometry subjects, and the performances were high in training (0.776 [95%CI, 0.746–0.810]), internal (0.767 [95%CI, 0.718–0.815]) and external validation (0.699 [95%CI, 0.633–0.766]) cohorts. In our radiomics signature, the majority of the features were transformed by wavelet filter, splitting imaging data into various different frequency components on three axis of the whole lung region [37]. This suggests that wavelet features probably interpret spatial heterogeneity in whole lung regions at multiple scales. In addition, the constructed radiomics signature model was combined with the clinical factors. Lu et al. predicted PRISm from the normal by the combination of CT quantitative parameters, as well as clinical features with an AUC of 0.786 [38]. Our study made a greater performance sightly (AUC = 0.787).

The constructed novel PRISm prediction nomogram was further evaluated by a decision curve to clarify the clinical utility, which could offer insight into clinical outcomes on the basis of threshold probability, from which the net benefit could be derived [39, 40]. The results showed that if the threshold probability of a patient is > 4%, the application of our constructed radiomics nomogram in predicting PRISm was more beneficial in relative to the treat-none or treat-all-patients scheme. The present novel nomogram provides an important quantitative indicator and reference for the decision-making and management of treatment regimens for PRISm subjects. The new approach sheds more lights on clinical outcomes according to threshold probability, and net benefits were obtained on this basis [41].

However, this study still has the following limitations. First, owing to the retrospective and multi-institutional nature of the current work, CT acquisition parameters and reconstruction techniques were not in consistence. But, we use techniques such as regularization, normalization, and resampling to improve the performance of CT images, thereby enhancing the accuracy and reliability of diagnosis. Second, common CT quantitative parameters can be measured to provide more information on pulmonary lesions, such as air trapping, pulmonary vascular disease and so on. Therefore, in the future, we will incorporate these common quantitative features to optimize our prediction model. Thirdly, to keep pace with the advances in technology, other advanced deep-learning algorithm should be applied in our further studies. Fourth, we have excluded lung cancer patients in this study; however, in future research, we will include lung cancer patients and apply whole lung radiomics to distinguish whether they have PRISm or not.

To sum up, the CT radiomics model incorporating clinical factors and radiomics signature is established and validated to identify PRISm in non-COPD subjects. The radiomics approach may be helpful to delay initiation COPD progression.

Abbreviations

COPD	Chronic obstructive pulmonary disease
GOLD	Global initiative for chronic obstructive lung disease
PFT	Pulmonary function test
FEV1/FVC	The ratio of forced expiratory volume in 1 s to forced vital capacity
PRISm	Preserved Ratio Impaired Spirometry
AFL	Airflow limitation
CT	Computed tomography
ROI	Region of interest
BMI	Body mass index
GLCM	Gray level cooccurrence matrix
GLSZM	Gray level size zone matrix
GLDM	Gray level dependence matrix
mRMR	Maximal redundancy minimal relevance
LASSO	Least absolute shrinkage and selection operator
DCA	Decision curves analysis
AUC	The area under the curve
ROC	The receiver operating characteristic curve

Supplementary Information

The online version contains supplementary material available at https://doi.org/10.1186/s12931-024-02964-2.

Supplementary Material 1

Acknowledgements
We thank the colleagues in our department for their help in our study.

Author contributions
TaoHu Zhou and Li Fan had full access to all of the data in the study and takes responsibility for the integrity of the data and the accuracy of the data analysis. Yu Guan and XiaoQing Lin contributed equally to this work. Concept and design: TaoHu Zhou and Li Fan. Acquisition, analysis, or interpretation of data: XiuXiu Zhou, Liang Mao, YanQing Ma, Bing Fan, Jie LiDrafting of the manuscript: TaoHu Zhou, Yu Guan and XiaoQing Lin. Statistical analysis: TaoHu Zhou. Obtained funding: ShiYuan Liu, Li Fan. Supervision: ShiYuan Liu, Li Fan. Image processing: TaoHu Zhou.

Funding
This work was supported by the National Key Research and Development Program of China (2022YFC2010002, 2022YFC2010000 and 2022YFC2010005), the National Natural Science Foundation of China (82171926, 81930049 and 82430065), the Medical Imaging Database Construction Program of National Health Commission (YXFSC2022JJSJ002), the Clinical Innovative Project of Shanghai Changzheng Hospital (2020YLCYJY24), the Program of Science and Technology Commission of Shanghai Municipality (21DZ2202600), and the Shanghai Sailing Program (20YF1449000).

Data availability
No datasets were generated or analysed during the current study.

Declarations

Ethics approval and consent to participate
This retrospective study involving human participants were reviewed and approved by the ethics committee of Second Affiliated Hospital of Naval Medical University. Patient informed consent was waived.

Consent for publication
No individual participant data is reported that would require consent to publish from the participant (or legal parent or guardian for children).

Competing interests
The authors declare no competing interests.

Author details
[1]Department of Radiology, Second Affiliated Hospital of Naval Medical University, No. 415 Fengyang Road, Shanghai 200003, China
[2]School of Medical Imaging, Shandong Second Medical University, Weifang 261053, Shandong, China
[3]College of Health Sciences and Engineering, University of Shanghai for Science and Technology, No.516 Jungong Road, Shanghai 200093, China
[4]Department of Medical Imaging, Affiliated Hospital of Ji Ning Medical University, Ji Ning 272000, China
[5]Department of Radiology, Zhejiang Provincial People's Hospital, Affiliated People's Hospital of Hangzhou Medical College, Hangzhou, ZJ, China
[6]Department of Radiology, Jiangxi Provincial People's Hospital, The First Affiliated Hospital of Nanchang Medical College, Nanchang, China

Received: 11 March 2024 / Accepted: 28 August 2024
Published online: 03 September 2024

References

1. Yin P, Wu J, Wang L, et al. The Burden of COPD in China and its provinces: findings from the global burden of Disease Study 2019. Front Public Health. 2022;10:859499. https://doi.org/10.3389/fpubh.2022.859499.
2. Yadav AK, Gu W, Zhang T, Xu X, Yu L. Current perspectives on Biological Therapy for COPD. Copd. 2023;20(1):197–209. https://doi.org/10.1080/15412555.2023.2187210.
3. Wang C, Xu J, Yang L, et al. Prevalence and risk factors of chronic obstructive pulmonary disease in China (the China Pulmonary Health [CPH] study): a national cross-sectional study. Lancet. 2018;28(10131):1706–17. https://doi.org/10.1016/s0140-6736(18)30841-9.
4. China. https://www.stats.gov.cn/
5. Al Wachami N, Guennouni M, Iderdar Y, et al. Estimating the global prevalence of chronic obstructive pulmonary disease (COPD): a systematic review and meta-analysis. BMC Public Health. 2024;25(1):297. https://doi.org/10.1186/s12889-024-17686-9.
6. Chen S, Kuhn M, Prettner K, et al. The global economic burden of chronic obstructive pulmonary disease for 204 countries and territories in 2020-50: a health-augmented macroeconomic modelling study. Lancet Glob Health. 2023;11(8):e1183–93. https://doi.org/10.1016/s2214-109x(23)00217-6.
7. Higbee DH, Granell R, Davey Smith G, Dodd JW. Prevalence, risk factors, and clinical implications of preserved ratio impaired spirometry: a UK Biobank cohort analysis. Lancet Respir Med. 2022;10(2):149–57. https://doi.org/10.1016/s2213-2600(21)00369-6.
8. Wan ES. The clinical spectrum of PRISm. Am J Respir Crit Care Med. 2022;1(5):524–5. https://doi.org/10.1164/rccm.202205-0965ED.
9. Park HJ, Byun MK, Rhee CK, Kim K, Kim HJ, Yoo KH. Significant predictors of medically diagnosed chronic obstructive pulmonary disease in patients with preserved ratio impaired spirometry: a 3-year cohort study. Respir Res. 2018;24(1):185. https://doi.org/10.1186/s12931-018-0896-7.
10. Wan ES, Fortis S, Regan EA, et al. Longitudinal phenotypes and mortality in preserved ratio impaired spirometry in the COPDGene Study. Am J Respir Crit Care Med. 2018;1(11):1397–405. https://doi.org/10.1164/rccm.201804-0663OC.
11. Wan ES, Hokanson JE, Regan EA, et al. Significant spirometric transitions and preserved ratio impaired Spirometry among ever smokers. Chest. 2022;161(3):651–61. https://doi.org/10.1016/j.chest.2021.09.021.
12. Wijnant SRA, De Roos E, Kavousi M, et al. Trajectory and mortality of preserved ratio impaired spirometry: the Rotterdam Study. Eur Respir J. 2020;55(1). https://doi.org/10.1183/13993003.01217-2019.
13. Washio Y, Sakata S, Fukuyama S, et al. Risks of mortality and airflow limitation in Japanese individuals with preserved ratio impaired spirometry. Am J Respir Crit Care Med. 2022;1(5):563–72. https://doi.org/10.1164/rccm.202110-2302OC.
14. Tong H, Cong S, Fang LW, et al. [Performance of pulmonary function test in people aged 40 years and above in China, 2019–2020]. Zhonghua Liu Xing Bing Xue Za Zhi. 2023;10(5):727–34. https://doi.org/10.3760/cma.j.cn112338-20230202-00051.
15. Oudkerk M, Liu S, Heuvelmans MA, Walter JE, Field JK. Lung cancer LDCT screening and mortality reduction - evidence, pitfalls and future perspectives. Nat Rev Clin Oncol. 2021;18(3):135–51. https://doi.org/10.1038/s41571-020-00432-6.
16. Sunyi Zheng, Peter MA, van Ooijen OM. Lung Cancer Screening and Nodule Detection: the role of Artificial Intelligence Artificial Intelligence in cardiothoracic imaging. 2020:459. https://doi.org/10.1007/978-3-030-92087-6_43
17. Gillies RJ, Kinahan PE, Hricak H. Radiomics: images are more than pictures, they are data. Radiol. 2016;278(2):563–77. https://doi.org/10.1148/radiol.2015151169.
18. Huang W, Deng H, Li Z, et al. Baseline whole-lung CT features deriving from deep learning and radiomics: prediction of benign and malignant pulmonary ground-glass nodules. Front Oncol. 2023;13:1255007. https://doi.org/10.3389/fonc.2023.1255007.
19. Huang W, Zhang H, Ge Y, et al. Radiomics-based machine learning methods for volume doubling time prediction of Pulmonary Ground-glass nodules with baseline chest computed Tomography. J Thorac Imaging. 2023;1(5):304–14. https://doi.org/10.1097/rti.0000000000000725.
20. Tu W, Sun G, Fan L, et al. Radiomics signature: a potential and incremental predictor for EGFR mutation status in NSCLC patients, comparison with CT morphology. Lung Cancer. 2019;132:28–35. https://doi.org/10.1016/j.lungcan.2019.03.025.
21. Wang Y, Lyu D, Fan L, Liu S. Advances in the prediction of spread through air spaces with imaging in lung cancer: a narrative review. Transl Cancer Res. 2023;31(3):624–30. https://doi.org/10.21037/tcr-22-2593.
22. Zhou T, Tu W, Dong P et al. CT-Based Radiomic Nomogram for the Prediction of Chronic Obstructive Pulmonary Disease in Patients with Lung cancer. Acad Radiol. 14. 2023;https://doi.org/10.1016/j.acra.2023.03.021

23. Agustí A, Celli BR, Criner GJ, et al. Global Initiative for Chronic Obstructive Lung Disease 2023 Report: GOLD Executive Summary. Eur Respir J. 2023;61(4). https://doi.org/10.1183/13993003.00239-2023.
24. Hofmanninger J, Prayer F, Pan J, Röhrich S, Prosch H, Langs G. Automatic lung segmentation in routine imaging is primarily a data diversity problem, not a methodology problem. Eur Radiol Exp. 2020;20(1):50. https://doi.org/10.1186/s41747-020-00173-2.
25. Yang K, Yang Y, Kang Y, et al. The value of radiomic features in chronic obstructive pulmonary disease assessment: a prospective study. Clin Radiol. 2022;77(6):e466–72. https://doi.org/10.1016/j.crad.2022.02.015.
26. Remeseiro B, Bolon-Canedo V. A review of feature selection methods in medical applications. Comput Biol Med. 2019;112:103375. https://doi.org/10.1016/j.compbiomed.2019.103375.
27. Guerra S, Carsin AE, Keidel D, et al. Health-related quality of life and risk factors associated with spirometric restriction. Eur Respir J. 2017;49(5). https://doi.org/10.1183/13993003.02096-2016.
28. Wan ES, Castaldi PJ, Cho MH, et al. Epidemiology, genetics, and subtyping of preserved ratio impaired spirometry (PRISm) in COPDGene. Respir Res. 2014;6(1):89. https://doi.org/10.1186/s12931-014-0089-y.
29. Maclay JD, MacNee W. Cardiovascular disease in COPD: mechanisms. Chest. 2013;143(3):798–807. https://doi.org/10.1378/chest.12-0938.
30. Guerra S, Sherrill DL, Venker C, Ceccato CM, Halonen M, Martinez FD. Morbidity and mortality associated with the restrictive spirometric pattern: a longitudinal study. Thorax. 2010;65(6):499–504. https://doi.org/10.1136/thx.2009.126052.
31. Mannino DM, McBurnie MA, Tan W, et al. Restricted spirometry in the Burden of Lung Disease Study. Int J Tuberc Lung Dis. 2012;16(10):1405–11. https://doi.org/10.5588/ijtld.12.0054.
32. Wei X, Ding Q, Yu N, et al. Imaging Features of Chronic Bronchitis with preserved ratio and impaired spirometry (PRISm). Lung. 2018;196(6):649–58. https://doi.org/10.1007/s00408-018-0162-2.
33. Yang Y, Li W, Guo Y, et al. Early COPD risk decision for adults aged from 40 to 79 years based on lung Radiomics features. Front Med (Lausanne). 2022;9:845286. https://doi.org/10.3389/fmed.2022.845286.
34. Yang Y, Li W, Guo Y, et al. Lung radiomics features for characterizing and classifying COPD stage based on feature combination strategy and multi-layer perceptron classifier. Math Biosci Eng. 2022;25(8):7826–55. https://doi.org/10.3934/mbe.2022366.
35. Yang Y, Li W, Kang Y, et al. A novel lung radiomics feature for characterizing resting heart rate and COPD stage evolution based on radiomics feature combination strategy. Math Biosci Eng. 2022;17(4):4145–65. https://doi.org/10.3934/mbe.2022191.
36. Yang Y, Wang S, Zeng N, et al. Lung Radiomics features selection for COPD Stage classification based on Auto-Metric graph neural network. Diagnostics (Basel). 2022;20(10). https://doi.org/10.3390/diagnostics12102274.
37. Wilson R, Devaraj A. Radiomics of pulmonary nodules and lung cancer. Transl Lung Cancer Res. 2017;6(1):86–91. https://doi.org/10.21037/tlcr.2017.01.04.
38. Lu J, Ge H, Qi L, et al. Subtyping preserved ratio impaired spirometry (PRISm) by using quantitative HRCT imaging characteristics. Respir Res. 2022;11(1):309. https://doi.org/10.1186/s12931-022-02113-7.
39. Localio AR, Goodman S. Beyond the usual prediction accuracy metrics: reporting results for clinical decision making. Ann intern med. 2012;157(4):294-5. https://doi.org/10.7326/0003-4819-157-4-201208210-00014
40. Van Calster B, Vickers AJ. Calibration of risk prediction models: impact on decision-analytic performance. Med Decis Mak. 2015;35(2):162–9. https://doi.org/10.1177/0272989x14547233.
41. Balachandran VP, Gonen M, Smith JJ, DeMatteo RP. Nomograms in oncology: more than meets the eye. Lancet Oncol. 2015;16(4):e173–80. https://doi.org/10.1016/s1470-2045(14)71116-7.

Publisher's note